Journal of Computer-Aided Molecular Design **18:** 145–154, 2004.

Solvent effect on the synthesis of clarithromycin: A molecular dynamics study

Dilek Duran[1], Viktorya Aviyente[1] & Canan Baysal[2,*]
[1]*Chemistry Department, Faculty of Arts and Sciences, Bogazici University, Bebek 34342 Istanbul, Turkey*
[2]*Laboratory of Computational Biology, Faculty of Engineering and Natural Sciences, Sabanci University, Orhanlı, 34956 Tuzla, Istanbul, Turkey*

Received 26 May 2003; accepted in revised form 26 March 2004

Key words: clarithromycin, conformational analysis, macrolide antibiotics, molecular dynamics, solvent effect

Summary

Clarithromycin (6-*O*-methylerythromycin A) is a 14-membered macrolide antibiotic which is active *in vitro* against clinically important gram-positive and gram-negative bacteria. The selectivity of the methylation of the C-6 OH group is studied on erythromycin A derivatives. To understand the effect of the solvent on the methylation process, detailed molecular dynamics (MD) simulations are performed in pure DMSO, pure THF and DMSO:THF (1:1) mixture by using the anions at the C-6, C-11 and C-12 positions of 2′,4″-[*O*-bis(TMS)]erythromycin A 9-[*O*-(dimethylthexylsilyl)oxime] under the assumption that the anions are stable on the sub-nanosecond time scale. The conformations of the anions are not affected by the presence of the solvent mixture. The radial distribution functions are computed for the distribution of different solvent molecules around the 'O^-' of the anions. At distances shorter than 5 Å, DMSO molecules are found to cluster around the C-11 anion, whereas the anion at the C-12 position is surrounded by the THF molecules. The anion at the C-6 position is not blocked by the solvent molecules. The results are consistent with the experimental finding that the methylation yield at the latter position is increased in the presence of a DMSO:THF (1:1) solvent mixture. Thus, the effect of the solvent in enhancing the yield during the synthesis is not by changing the conformational properties of the anions, but rather by creating a suitable environment for methylation at the C-6 position.

Introduction

Clarithromycin (6-*O*-methylerythromycin A) is a 14-membered macrolide antibiotic which is active *in vitro* against clinically important gram-positive and gram-negative aerobes and anaerobes responsible for respiratory tract infections [1–5]. The effect of combining clarithromycin with a variety of other drugs for the treatment and prevention of disseminated *Mycobacterium avium* complex (MAC) infection in patients with AIDS is under investigation [6]. Clarithromycin exerts its antibacterial action by binding to the bacterial ribosome, specifically to the 50S unit. Recently, the high resolution X-ray structures of the 50S ribosomal subunit of the eubacterium *Deinococcus radiodurans*, complexed with erythromycin A and clarithromycin were determined [7].

Clarithromycin's chemical structure is identical to that of erythromycin A, except that the *O*-methyl group has been substituted for a hydroxy group at position C-6 of the lactone. The presence of the methoxy group makes the molecule more hydrophobic than erythromycin and improves the stability of erythromycin against acids. It also enhances its antibacterial and pharmacokinetic properties [8]. Several methods for the synthesis of clarithromycin have been published [9–14]. It was originally synthesized via methylation of 2′-*O*,3′-*N*-bis(benzyloxycarbonyl)-*N*-demethylerythromycin A, but low yields were reported because of the lower selectivity towards 6-*O*-methylation [10]. An improved process for the select-

*To whom correspondence should be addressed. Fax: +90 (216) 4839550; E-mail: canan@sabanciuniv.edu

ive methylation of a hydroxy group at position C-6 was achieved using 9-oxime erythromycin A and protecting the hydroxy group at positions 2′ and 4″ with an *O*-protecting group (chlorotrimethylsilane, TMS-Cl) [14]. This protected compound was allowed to react with methyl iodide (CH_3I) and potassium hydroxide (KOH) in a mixture of dimethylsulfoxide (DMSO) and tetrahydrofuran (THF) (1:1); this approach resulted in a yield of 56% (Scheme 1).

In our previous work [15], starting with the 9-[*O*-(dimethylthexylsilyl)oxime] derivative of erythromycin A, the protection of each hydroxy group in the macrolide with TMS-Cl was modeled in vacuum. Furthermore, the selectivity of the 6-*O*-methylation was investigated using the 2′,4″-[*O*-bis(trimethylsilyl)]erythromycin A 9-[*O*-(dimethylthexylsilyl)oxime]. In the presence of a bulky derivative of an oxime group (9-[*O*-(dimethylthexylsilyl)]) the hydroxy groups at positions C-11 and C-12 were automatically protected against the attack of the methylating reagent (CH_3I) and the hydroxy group at position C-6 was methylated. The structures proposed as well as the methodology used reproduced the experimental findings and paved the way to study the reaction mechanisms of other 14-membered macrolides [16,17]. On the other hand, the type of solvent used as the reaction medium may be detrimental in the final products and yields obtained. For example, Watanabe et al. [10] have shown, using a variety of protecting groups, that the selectivity of 6-*O*-methylation can be enhanced by modulating the solvent. Therein, methylation was not observed in pure tetrahydrofuran (THF), whereas a 63.7% yield was obtained in pure dimethyl sulfoxide (DMSO). They obtained a maximum yield of 86.2% when the reaction medium was a 1:1 mixture of DMSO and THF.

Macrocyclization is a process commonly employed in nature for molecules to display bioactivity [18]. The constraints imposed by the formation of a ring greatly reduce the number of conformations that may be sampled by the molecule. Typically only one or a few significantly different conformations will be accessible at relevant temperatures [19, 20], making it relatively simple for the molecule to achieve its active conformation when it is presented to the site where it will function. Experimental evidence for erythromycin A and its derivatives (eg. clarithromycin, dirithromycin, roxithromycin) from the crystal structures as well as nuclear magnetic resonance data in solution show that the backbone conformation is unique for these 14-membered macrolides; differences in side-chain conformers do exist [21–24]. In light of these experimental findings, it seems plausible that the backbone conformation of this particular family of macrolides is very stable and that different solvents will not affect the conformations unless very strong solvent–solute interactions are created. The side chains are expected to be more open to conformational changes in different solvents, however, so that a particular side-chain may block the methylation site in certain conformers and prevent the reaction, in effect changing the reaction yield. An alternative way by which the solvent may accompany the reaction is by creating highly favorable interactions between the solvent and the methylation site. In this case, it requires a high energy for the methylating reagent to displace the solvent molecules and enter the favorable positioning for the reaction to occur.

In this study, we seek to understand the molecular basis of why high yields for 6-*O*-methylation is obtained in certain solvents. For this purpose, we carry out molecular dynamics (MD) simulations on the C-6, C-11, and C-12 anions of 2′,4″-[*O*-bis(trimethylsilyl)]erythromycin A 9-[*O*-(dimethylthexylsilyl)oxime] in pure DMSO, in pure THF, and in DMSO:THF (1:1) solution, based on the assumption that the anions are stable on the subnanosecond time scale in these solvents. We gain insight into how the presence of the solvent affects the methylation process by performing (i) a detailed conformational analysis; and (ii) studying the distribution of solvent molecules around the methylation sites.

Methodology

MD simulations were performed for the anions at the C-6, C-11 and C-12 positions of 2′,4″-[*O*-bis(trimethylsilyl)]erythromycin A 9-[*O*-(dimethylthexylsilyl) oxime] using the Molecular Simulations Inc. InsightII 98.0 software package [25]. The starting conformations were taken from the previous study [15], where the molecules were optimized with AM1 method in GAUSSIAN 98 [26].

Each starting conformation was first solvated in a periodic cubic box with THF and DMSO solvent mixture, pure DMSO and pure THF molecules using Amorphous Cell Module Version 10.0 [25]. All the solvent atoms were treated explicitly. The number of solvent molecules was set according to the experimental conditions, DMSO:THF (1:1), DMSO and THF by using their densities ($d_{\mathrm{DMSO}} = 1.14$ g/cm^3,

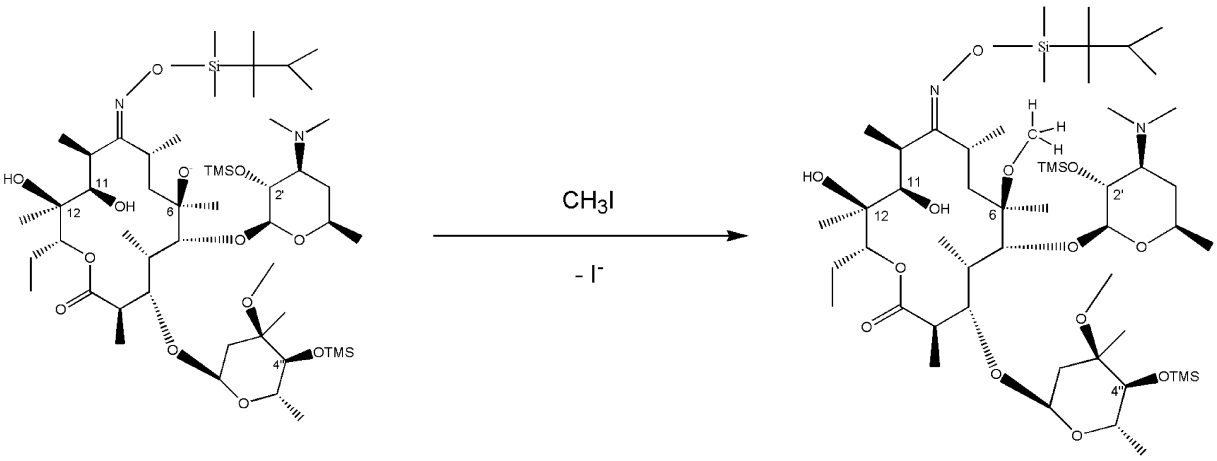

Scheme 1.

$d_{THF} = 0.88$ g/cm^3 at 25 °C). For DMSO:THF (1:1), this resulted in 350 THF and 416 DMSO molecules placed around each structure in a cubic box, whereas 717 and 900 solvent molecules were placed around each structure for pure THF and DMSO, respectively. The cubic box has a length of 45.8, 46.3, and 47.6 Å on each side in the respective cases. The systems were minimized through 200 steps by the steepest descent method using the Consistent Valence Force Field (CVFF) [27]. At this initial optimization stage, the nonbonded interactions were treated with a simple 8.5 Å atom-based cutoff distance; a switching function was used with the buffer width set to 0.5 Å. We thus prepared a starting structure for the MD simulation of each of the three anions in each of the three solvent environments, leading to 9 initial structures prepared for subsequent MD runs.

In each system, the Discover program was used with CVFF. MD simulations were carried out at 298 K using the temperature control method of Andersen [28]. Initial velocities were generated from a Boltzmann distribution at an average temperature of 298 K. Newton's equations of motion were integrated with the Verlet algorithm [28, 29]. The nonbonded interactions were treated with a simple 15 Å atom-based cutoff distance; a switching function was used with the buffer width set to 0.5 Å. After energy minimization, 600 ps of MD simulation was run at 298 K whose first 100 ps corresponds to the equilibration stage followed by 500 ps of data collection. A 600 ps simulation takes approximately 37 days of CPU time on a Silicon Graphics O2 workstation with a 360-MHz R12000 CPU and 2048 Mb RAM. The long computing time is a result of the large cutoff distance of 15 Å used due to the presence of the explicit charge that participates in long-range interactions; thus, interactions between a substantially larger number of nonbonded pairs are computed compared to simulations where a more conventional cutoff of ca. 10 Å is used. The solute coordinates were saved every 1 ps during the production stages, thus resulting in 500 snapshots for each anion.

Results

Conformational analysis

MD runs were made on the anions at the C-6, C-11 and C-12 positions of the 2′,4″-[*O*-bis(trimethylsilyl)]erythromycin A 9-[*O*-(dimethylthexylsilyl)oxime]. During the MD simulation of each anion, 500 different structures were recorded from the data collection stage. Since the starting structures were taken as the optimized ones from AM1 calculations, we first check if the 100 ps equilibration period is adequate for the molecules to settle into their equilibrium conformations dictated by the solvent environment. Trajectories of selected dihedral angles of the anions were monitored for this purpose. For each anion, all 14 dihedral angles on the backbone (ϕ_n) as well as eight dihedral angles on the side chains (χ_n), which may influence the conformation of the backbone, were considered in the analysis. These angles are shown schematically in Figure 1. We find that all the 22 dihedral angles that were monitored fluctuate within ca. $\pm 10°$ of their average value; i.e. after 100 ps, the molecules attain their new equilibrium state.

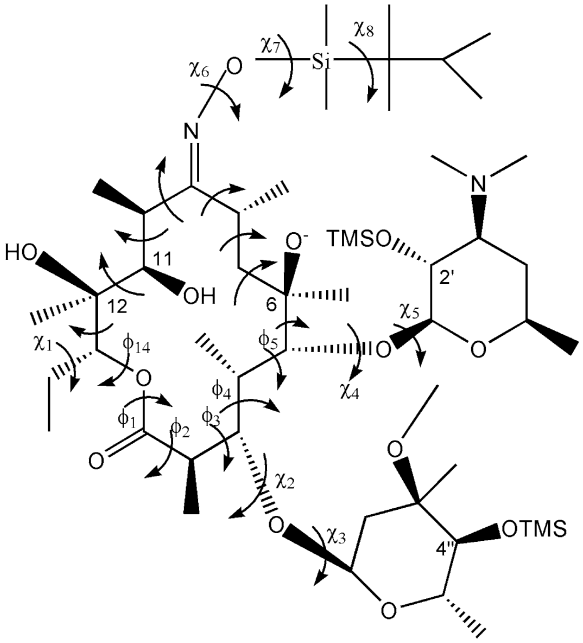

Figure 1. Essential dihedral angles defining the conformation of the anion. 14 dihedrals from the backbone (ϕ_1–ϕ_{14}), and 8 dihedrals from the side-chains (χ_1–χ_8) are selected. The C-6 anion is shown here; the dihedrals in the C-11 and C-12 anions follow the same numbering scheme.

We next compare the average structures with the optimized ones from our previous work [15] to discern the effect of solvent on molecular conformations. The detailed comparison is given in the supplementary material for the C-6, C-11, and C-12 anions. We define the angles to be significantly different if the difference between the value of the dihedral from the optimized structure and that from the MD simulation is larger than 30° on the backbone and 60° on the side-chains. The larger value chosen for the latter is due to the less constrained nature of these bonds. We find that once equilibrium is established, all the conformationally important angles in the C-11 and C-12 anions fluctuate close to the optimized value, irrespective of the solvent medium. In fact, to a good approximation, the optimal structure is within the bounds of the fluctuations of the dynamics for these two anions. On the other hand, the C-6 anion displays few differences between the optimized structure in vacuum and the stable structure in solvent. In particular, the ϕ_3 dihedral angle on the backbone ring is rotated from −141° in vacuum to −65° in the DMSO:THF (1:1) mixture, −89° in DMSO and −72° in THF. Note that this large rotation of ca. 70° is balanced by counter-rotations of ca. 25° in the ϕ_1 and ϕ_5 angles. The χ_7 dihedral on the oxime is also rotated from 140° in vacuum to 67° in the mixture, −173° in DMSO and −148° in THF.

We have made two control runs to understand the differences between the optimized structure and MD runs of the C-6 anion. First, we have optimized the final structure in the MD simulation in the gas phase with the AM1 method, using the same procedures as in our previous work [15], to make sure we did not miss a global minimum during the conformational search. We confirm that the new structure is at a local minimum, located 3 kcal/mol above the global minimum. Note that we can go so far as to *assume* that the lowest energy structure obtained from the conformational search performed in our earlier work is the global energy minimum (GEM). In general for cyclic molecules of the current size, it is relatively easy to locate the GEM using standard conformational search methods [30], one of which is the high temperature MD approach we used earlier [15, 17]. Next, we performed an MD simulation of the C-6 anion *in vacuo*, starting from the optimized structure. We checked the average values of the dihedral angles and their fluctuations as before (data not displayed). The results showed that these values are all similar to those obtained from the MD simulation of the C-6 anion in the solvent. In particular, the average values of the ϕ_1, ϕ_3, ϕ_5, and χ_7 dihedral angles are 175, −88, −66, and 62°, respectively. We thus conclude that the conformational differences observed in the C-6 anion are not due to the presence of the solvent, but that the vacuum-optimized structure of the C-6 anion is not stable in a dynamic environment and rapidly escapes to the more stable conformation within the first 100 ps of the simulation. In other words, the entropic effect cannot be ignored so that the global energy minimum and the global free energy minimum, are different [31]. Notice that the Helmholtz free energy surface, rather than the internal energy surface, is sampled in the MD trajectories.

The analysis carried out so far demonstrates that the solvent does not change the overall conformations of the C-6, C-11, and the C-12 anions in a manner that will affect the accessibility of the anions for methylation, except for the C-6 anion in THF (see below). Note that the conformations of the anions, although very similar to each other, are not the same. Setting aside some differences along the side chains, the C-11 and C-12 anions have the same backbone conformation. C-6 differs from these two at the ϕ_8, ϕ_9, and ϕ_{10} dihedrals by ca. −60, 165, and −170°, respectively, in all solvents studied. Such changes in the dihedrals directly affect the positioning of the oxime

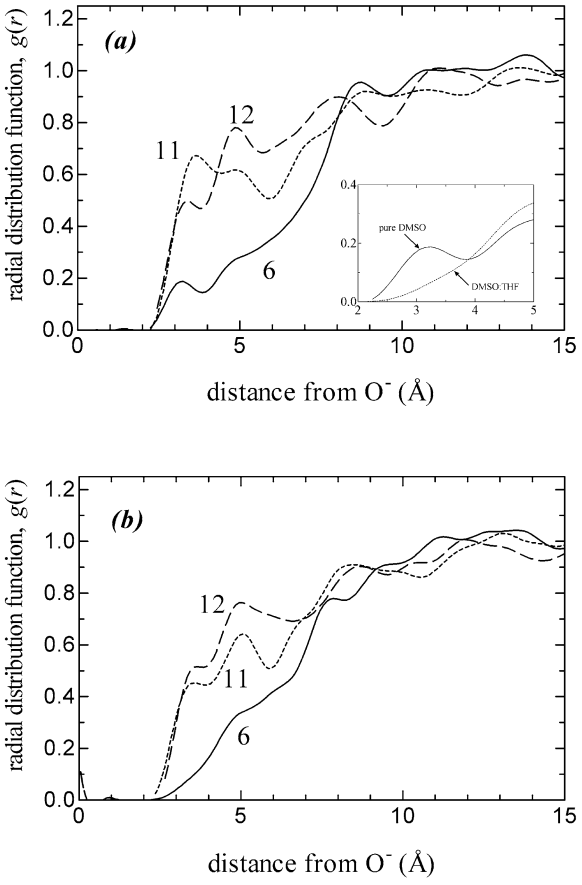

Figure 2. Radial distribution functions (RDFs), $g(r)$, for the distribution of the solvent molecules around the O^- of the anions at the C-6, C-11 and C-12 positions; (a) the solvent is pure DMSO; (b) the solvent is a DMSO:THF (1:1) mixture. Both solvents cluster around the C-11 and C-12 anions, and the C-6 anion is not blocked at short distances. Inset to (a): RDFs of the two types of solvent around the C-6 anion at distances less than 5 Å. There is a small peak at 3.2 Å in pure DMSO. This slight preference explains the corresponding slight decrease in the methylation yield; see text for details.

group, which in turn may affect the accessibility of the methylation site. In fact, the slight differences (10–20°) in the ϕ_3, χ_3, χ_6, χ_7, and χ_8 dihedrals of the system in pure THF affect the positioning of the methyl groups and TMS at C-4″ on the side chains. This restricts the accessibility of the C-6 position by both the solvent molecules and the methylating agent, and completely prevents its methylation. For the other solvents, such prohibitive conformational changes do not occur. To quantify the accessibility of the O^- atom, we computed the accessible surface area using the definition of Richards [32]. We computed the radii of the DMSO and THF molecules using an *ab initio* method in GAUSSIAN 98 [26] and found the radii of both as 3.8 Å; with the same methodology we calculated the radius of the methylating agent, CH_3I, as 3.7 Å. We therefore use a probe radius of 3.8 Å in our calculations of the accessible surface area. We find that the accessibility of the C-11 anion is ca. 8.5 ± 0.5 Å and that of the C-12 anion is ca. 9.5 ± 0.5 Å in all solvents. On the other hand, the accessibility of the C-6 anion is 0 in THF, whereas it is ca. 3.5 ± 0.5 Å in DMSO and the mixture.

Since it has been shown previously that the methylation yield of 2′,4″-[*O*-bis(trimethylsilyl)]erythromycin A 9-[*O*-(dimethylthexylsilyl)oxime] depends largely on the type and concentration of the solvent [14], other factors must be influencing the yield. We next analyze the structure of the solvent around the methylation site to obtain a deeper understanding of the processes involved.

Solvent effect on local environment

To understand the molecular basis of the solvent effect, the radial distribution functions (RDFs) were computed for the distribution of the solvent molecules around the 'O^-' of the anions. The RDF, $g_{ij}(r)$, is given by $g_{ij}(r) = \rho_{ij}(r) / <\rho_j>$, where $\rho_{ij}(r)$ is the number density of atom j at a distance r from an atom i, and $<\rho_j>$ is the average number density of atom j. The $g_{ij}(r)$ are averaged over the 500 recorded snapshots of each trajectory. We reproduced the RDFs for various atoms of the solvent molecules, i.e. S and C atoms in DMSO and C and O atoms in THF. We confirm that the general findings of the study do not change by this choice. Below, the RDFs of the anion oxygen distances in any direction from a central solvent molecule are shown, where the S is taken as the central atom of DMSO and O is taken for THF. Since the number of conformations we average over is relatively small (500 snapshots), we apply a third degree, five-point smoothing to the data [33].

The calculated RDFs are shown in Figure 2 for the structure of the solvent around the three anions; the distributions of the solvent molecules are shown for pure DMSO and the DMSO:THF (1:1) mixture in parts a and b, respectively. The results for the C-11 and C-12 anions in THF are very similar to the data in pure DMSO; for the C-6 anion, the accessibility of this location is prevented by a conformational change in the side chain angles, as discussed in the previous section. We therefore do not include the radial distribution functions for the systems in THF.

We find that the solvent density approaches the bulk value ($g(r) \rightarrow 1$) at distances of ca. 8 Å in all three cases and in both solvents. On the other hand, at distances shorter than ca. 6 Å, the solvent molecules cluster predominantly around the O^- of the C-11 and C-12 anions ($g(r) > 0.6$) in both cases, as opposed to the O^- of the C-6 anion which has very little to no exposure to the solvent at these distances ($g(r) < 0.2$). In other words, there are no prevailing favorable interactions between the solvent and the anion in the latter case, so that methylation may proceed smoothly at this site. Conversely, the solvent molecules tend to cluster around the C-11 and C-12 anions and prevent the methylating agent to approach these sites.

Experimental findings also show that the 6-O methylation yield is somewhat higher in the presence of a DMSO:THF (1:1) solvent mixture compared to pure DMSO [10]. Shown in the inset to Figure 2a is the RDF of the solvent molecules around the C-6 anion at distances less than 5 Å. Although the number density of solvent molecules around this anion is very small in both solvents, we find that there is a small peak at 3.2 Å in pure DMSO, whereas this peak does not exist in the solvent mixture. We conclude that the DMSO molecules tend to block this anion to some extent, and prevent methylation from proceeding at higher yields. Since the conformation of the molecule is indifferent in both types of solvents (see Supplementary Material for details of the average conformations), specific interactions between THF and DMSO molecules must be preventing the solvent molecules from clustering around the C-6 O^- in the DMSO:THF (1:1), paving the way for the methylating agent to approach the anion.

We further compute the separate RDFs of DMSO and THF molecules around the anions in the DMSO:THF (1:1) mixture; these results are shown in Figure 3a and 3b, respectively. The DMSO molecules cluster predominantly around the O^- of the C-11 anion. As displayed in Figure 3a, they have a first coordination shell with a peak at 4.8 Å and a second, more populated coordination shell with a peak at 8.3 Å. Compared to the C-11 anion, DMSO molecules show much less clustering around the C-6 and C-12 anions. On the other hand, the THF molecules have an affinity for the C-12 site. As shown in Figure 3b, there is a broad first coordination shell peaking at 4.9 Å. The affinity of THF for the C-11 anion is lower than that of C-12, showing two peaks at 3.4 and 5.2 Å. There is no significant population of THF molecules around the C-6 anion. Thus, at distances

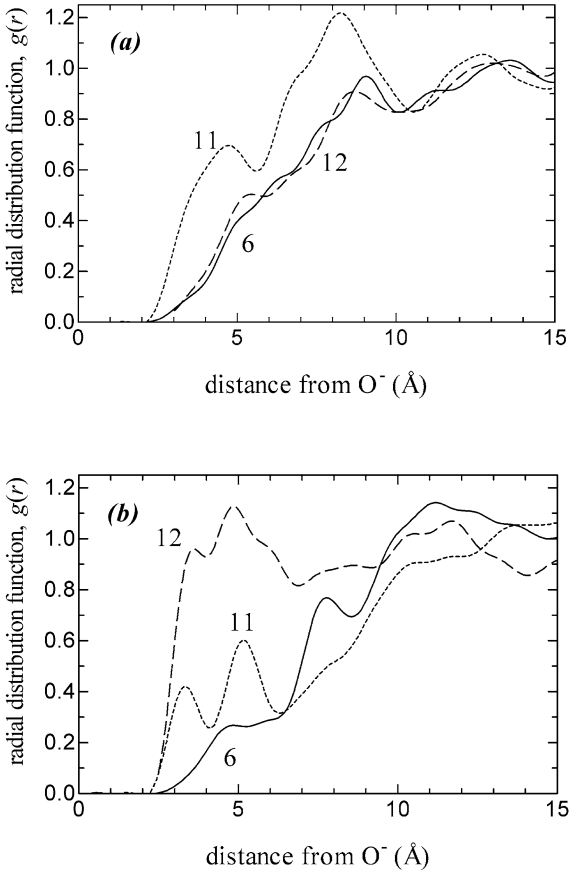

Figure 3. Radial distribution functions (RDFs), $g(r)$, for the distribution of the different types of solvent molecules in the DMSO:THF (1:1) mixture around the O^- of the anions at the C-6, C-11 and C-12 positions; (a) DMSO molecules; (b) THF molecules. DMSO clusters around the C-11 anion, whereas THF clusters around the C-12 anion.

shorter than 5 Å, there is a substantial organization of DMSO molecules around the C-11 anion and THF molecules around the C-12 anion in DMSO:THF (1:1) mixture. Since DMSO and THF molecules can fit cavities of the same size (the effective radius is 3.8 Å for both), their preference for different sites is concluded to be due to specific interactions.

Mechanisms of solvent obstruction from small molecule models

To gain insight into the results of RDFs of the anions with the solvent molecules, the reactions of the anion with the solvent molecules, DMSO and THF, were explored for small model systems by using semi-empirical (AM1 and PM3) methods in the SPARTAN 5.1.3 program [34] and an ab initio method (B3LYP/6-

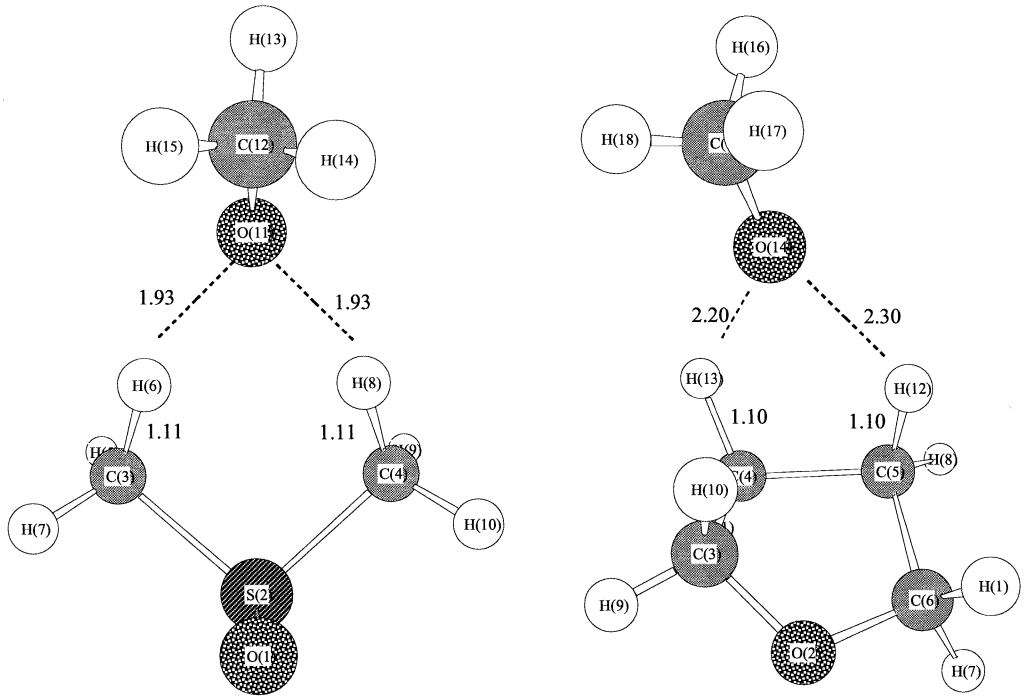

Figure 4. The optimized structures of the anions with the DMSO (1) and THF (2) molecules and the selected bond lengths (Å) are given for B3LYP/6-31+G**.

31+G**) in GAUSSIAN 98 [26] in vacuum. In the small models, the methoxy anion was used. The reactants and the products were fully optimized by the AM1, PM3 and B3LYP/6-31+G** methods (Table 1). The nature of the stationary geometries was confirmed by the presence of real vibrational frequencies. The distances (Å) of the anion oxygen with the solvent molecules and the heats of reaction (ΔE) between the reactants and the products were evaluated (Table 1).

Basis set superposition error (BSSE) occurs because the energy of each unit within an associated complex will be lowered by the basis functions of the others. BSSE introduces a nonphysical attraction between the two units. The counterpoise correction (CP) proposed by Boys and Bernardi [35] has been used to correct for BSSE, despite the fact that other methods for correcting this error have been discussed in the literature [36]. The CP method calculates each of the units with the basis functions of the other (but without the nuclei or electrons), using 'ghost orbitals'. The CP-corrected interaction energy, $E^{CP}_{\text{interaction}}$, is given in Equation 1:

$$E^{CP}_{\text{interaction}} = E_{\text{super}} - \sum_{i=1}^{n} E_{m^i_{opt}} + \sum_{i=1}^{n} (E_{mf} - E^*_{mf}) \quad (1)$$

where the E_m's represent the energies of the individual monomers [37]. The subscripts 'opt' and 'f' denote the individually optimized monomers and those frozen in their supermolecular geometries and the asterisk (*) denotes monomers calculated with ghost orbitals. The CP correction has been used to refine the energetics of the complexes in Table 1; as displayed, the BSSE corrected interaction energies reflect the same behavior as the non-corrected ones.

As shown in Figure 4, the anion forms a stable complex with DMSO as a six-membered ring (1); the bond distances between the hydrogen atoms and the oxygen of the anion are 1.93 Å. The complex of the anion with THF, on the other hand, forms a five-membered ring (2); the bond distances between the hydrogen of the carbon atoms and the oxygen are ca.

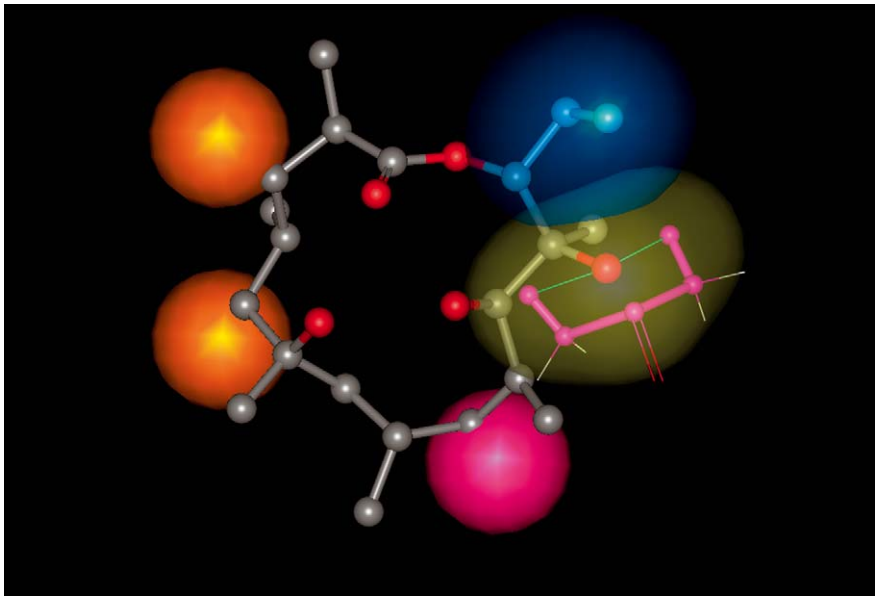

Figure 5. Snapshot from the MD trajectory of the C-12 anion in DMSO. The anion makes two favorable interactions with the hydrogen of the methyl groups on the DMSO molecule, forming a stable six-membered ring. For clarity of the presentation of the main ring, the sugar rings have been replaced by orange spheres and the 9-oxime group by a pink sphere. The volume occupied by the DMSO is shown in yellow. The blue region displays the solvent accessible surface area of the neighboring atoms, thereby showing how the approach of a second solvent molecule to the anion is prevented. The bond lengths (shown in green) between the O^- and the closest hydrogen atoms of the methyl groups in DMSO are 1.93 and 2.09 Å.

Table 1. Selected Bond Distances (Å) and the Energies (kcal/mol) for the formation of complexes with the DMSO and THF; BSSE corrected energies are presented in parentheses.

	AM1	PM3	B3LYP/6-31+G**
(O^-...DMSO'S)	3.359	3.605	3.764
ΔE	−18.12	−28.96	−21.43 (−20.09)
(O^-...THF'O)	4.747	4.417	4.274
ΔE	−8.34	−10.62	−11.91 (−10.99)

$\Delta E = \Delta E_{\text{product}} - \Delta E_{\text{reactants}}$.

2.2 Å. The results show that at distances shorter than 5 Å, both DMSO and THF molecules are capable of forming stable complexes with the anion and prevent methylation from occurring. Note that, irrespective of the level of theory used, anion–DMSO interactions are always more stable than anion–THF interactions. In general, a THF molecule would be easier to displace from around the anion than a DMSO molecule. However, the specific interactions in the larger system are much more complicated. This is exemplified by the preference of DMSO towards the C-11 and THF towards the C-12 anions, whereas none of the solvents prefer to be around the C-6 anion (Figures 2 and 3). One might raise the steric effects as the origin of these differences; however, although the C-12 anion is completely exposed to the solvent, it displays a preference for THF over DMSO (see Figure 3). Since the calculated radius of the methylating agent is 3.7 Å, steric effects will not be effective during its competition towards the anion with the solvent molecules, which are of a very similar size (3.8 Å).

Mechanisms of solvent obstruction from MD trajectories

We have further examined snapshots from the trajectories to understand the specific interactions between the solvent molecules and the anions. In each trajectory, distances up to the 5 Å region of the O^- were considered in detail. In this analysis, we define favorable O.....H interactions if the distance between the anion O^- and the solvent H atom is less than 3 Å. Of these 'favorable interactions', the stronger hydrogen bonds are defined for distances shorter than 2.7 Å and O....H–C angles greater than 140°. One such snapshot is displayed in Figure 5 for the interaction of the closest DMSO molecule with the C-12 anion, at the end of the trajectory from the MD simulation in pure DMSO. The stable configuration of the DMSO with

the anion molecule as inferred from the small molecule models mentioned in the previous subsection is reproduced exactly. Such stable configurations prevail throughout all the trajectories we have examined, with the closest THF molecules forming five-membered rings and DMSO molecules six-membered rings with the anion. Note that these are not trapped solvent molecules in the vicinity of the anion. In the dynamic environment, solvent molecules change their location; yet there are always favorable interactions as defined above between the solvent H atoms and the solute O^- during the transient from the destruction of a stable ring structure to the formation of a new one. In fact, sample snapshots from the trajectories of the C-11 and C-12 anions display the same complexes with THF and DMSO as in the small molecule models (see the previous subsection) upon optimization.

We have shown by the RDF between the anions in DMSO:THF (1:1) mixture, and the solvent molecules that DMSO molecules tend to cluster predominantly around the C-11 anion (Figure 3a). This can be observed in the snapshots of the trajectory of C-11 anion, where we only find DMSO molecules around the C-11 anion. The DMSO molecules form such a pattern that they predominantly form two favorable interactions with the hydrogens of the methyl groups on the nearest DMSO molecule, forming a stable six-membered ring. A hydrogen bond with the C-11 anion and a hydrogen of the methyl groups is also frequently observed. On the other hand, for the C-12 anion, our analysis of the RDFs has revealed that THF molecules cluster around the O^- (Figure 3b). In the detailed analysis of snapshots from the trajectory of the C-12 anion, we mainly find two favorable interactions between the hydrogens of the THF molecule and the anion to form a five-membered ring. As in the C-11 anion, a hydrogen bond with the C-12 anion and a hydrogen from the solvent molecules is also frequently observed. Finally, in the C-6 anion, neither type of solvent molecules form predominant favorable interactions with the anion.

For pure DMSO simulations, our analysis of the snapshots reveals that the six-membered ring system is prevalent with the C-11 and C-12 anions; occasionally, hydrogen bonding between solvent and solute is also observed. However, this type of interaction is very weak in the C-6 anion, where the solvent molecules are around the C-6 anion at an average distance of ca. 3.1 Å.

Conclusions

We have carried out MD simulations of the C-6, C-11 and C-12 anions of the 2′,4″-[*O*-bis(trimethylsilyl)]erythromycin A 9-[*O*-(dimethylthexylsilyl)oxime] in pure DMSO, pure THF, and DMSO:THF (1:1) solutions, based on the assumption that the average lifetimes of the anions are longer than the sub-nanosecond time scales studied here. These simulations allow a better understanding of the solvent effect on the methylation process.

We find that the conformers of the anions of these 9-oxime derivatives are very stable so that they fluctuate around the same minima irrespective of the environment studied here (i.e. vacuum and three different solvent environments). The conformations of the C-6, C-11 and C-12 anions are mildly affected by the presence of the solvent. Only in pure THF does the presence of solvent cause a conformational change that leads to a loss in the accessibility of the C-6 anion. In the other solvents, the calculations of the RDFs for the distribution of the solvent around the anions show that at distances shorter than 5 Å, the anions at the C-11 and C-12 positions are surrounded by the solvent molecules, whereas the anion at C-6 is not blocked (Figure 2). This arrangement of the system allows optimal conditions for the preferential methylation of the C-6 position [14]. In addition, there is some amount of obstruction around the C-6 anion in pure DMSO, which explains the experimentally observed small but significant enhancement of methylation yield at this site in DMSO:THF (1:1) mixture [10]. In the latter solvent, we find a higher affinity between DMSO – C-11 anion and THF – C-12 anion pairs (Figure 3). We have further carried out quantum mechanical calculations on small methoxy–solvent model systems and shown that the anion could form complexes with both types of solvent molecules at distances shorter than 5 Å. These complexes were found to prevail throughout the MD trajectories; yet, the exact complex that will form around a given anion appears due to a sensitive interplay between (i) steric effects operative in the immediate environment of the anion; (ii) the bulk effect of the solvent (forming a frictional environment as well as randomly colliding with the solute atoms); and (iii) specific interactions between the anion and the solvent molecules. The latter is found to be especially important in the current systems, shaped by the complex web of interactions that propagate throughout the solvent. Note that these solvent effects also control

the reaction kinetics by adjusting the barrier heights, hence affecting the reaction rate.

Acknowledgements

The authors would like to thank Boğaziçi Araştırma Fonu project 01M101 and TUBITAK (The Scientific and Technical Research Council of Turkey) Münir Birsel Foundation for financial support. We also thank Gungor Ozer and Cem Ozturk for their help on some technical problems.

References

1. Kurath, P., Jones, P.H., Egan R.S. and Perun, T.J., Experientia, 27 (1971) 362.
2. Morimoto, S., Takahashi, Y., Watanabe, Y. and Omura, S., J. Antibiot., 37 (1984) 187.
3. Morimoto, S., Misawa, Y., Adachi, T., Nagate, T., Watanabe Y. and Omura, S., J. Antibiot., 43 (1990) 286.
4. Morimoto, S., Nagate, T., Sugita, K., Ono, T., Numata, K., Miyachi, J., Misawa Y. and Yamada, K., J. Antibiot., 43 (1990) 295.
5. Atkins, P.J., Herbert T.O. and Jones, N.B., Int. J. Pharm., 30 (1986) 199.
6. van Rooyen, G.F., Smit, M.J., de Jager, A.D., Hundt, H.K.L., Swart, K.J. and Hundt, A.F., J. Chromatogr. B, 768 (2002) 223.
7. Schlunzen, F., Zarivach, R., Harms, J., Bashan, A., Tocilj, A., Albrecht, R. and Yonath, A., Nature, 413 (2001) 814.
8. Morimoto, S., Watanabe, Y., Omura S. and Takahashi, Y., J. Antibiot., 37 (1984) 187.
9. Watanabe, Y., Adachi, T., Asaka, T., Kashimura, M., Matsunaga T. and Morimoto, S., J. Antibiot., 46 (1993) 1163.
10. Watanabe, Y., Morimoto, S., Adachi, T., Kashimura M. and Asaka, T., J. Antibiot., 46 (1993) 647.
11. Watanabe, Y., Adachi, T., Asaka, T., Kashimura M. and Morimoto, S., Heterocycles, 31 (1990) 2121.
12. Watanabe, Y., Kashimura, M., Asaka, T., Adachi T. and Morimoto, S., Heterocycles, 36 (1993) 243.
13. Omura, S. Morimoto, S., Nagate, T., Adachi T. and Kohno, Y., Yakugaku Zasshi, 112 (1992) 593.
14. Allevi, P., Longo A. and Anastasia, M., Bioorg. Med. Chem., 7 (1999) 2749.
15. Duran, D., Aviyente, V., and Baysal, C., J. Chem. Soc., Perkin Trans. 2, 3 (2002) 670.
16. Duran, D., Aviyente, V. and Baysal, C., J. Mol. Model., 10 (2004) 94.
17. Duran, D., Aviyente, V. and Baysal, C., J. Comput.-Aided Mol. Design, 18 (2004).
18. Kohli, M.R., Walsh C.T. and Burkart, M.D., Nature, 418 (2002) 658.
19. Baysal C. and Meirovitch, H., Biopolymers, 50 (1999) 329.
20. Baysal C. and Meirovitch, H., Biopolymers, 53 (2000) 423.
21. Iwasaki, H., Sugawara, Y., Adachi, T., Morimoto S. and Watanabe, Y., Acta Crystallogr., C49 (1993) 1227.
22. Awan, A., Brennan, R.J., Regan A.C. and Barber, J., J. Chem. Soc., Perkin Trans. 2, (2000) 1645.
23. Benarous-Gharbi, J., Ladam, P., Delaforge M. and Girault, J.P., J. Chem. Soc., Perkin Trans. 2, (1993) 2303.
24. Luger P. and Maier, R., J. Cryst. Mol. Struct., 9 (1979) 329.
25. Molecular Simulations Inc., S.R., Waltham, San Diego, CA.
26. GAUSSIAN 98 Revision A.1; Frisch, M.J.T., Trucks, G.W., Schlegel, H.B., Scuseria, G.E., Robb, M.A., Cheeseman, J.R., Zakrzewski, V.G., Montgomery, J.A., Stratmann, R.E., Burant, J.C., Dapprich, S., Millam, J.M., Daniels, A.D., Kudin, K.N., Strain, M.C., Karkas, O., Tomasi, J., Barone, V., Cossi, M., Cammi, R., Mennucci, B., Pomelli, C., Adamo, C., Clifford, S., Ochterski, G., Petersson, G.A., Ayala, P.Y., Cui, Q., Morokuma, K., Malick, D.K., Rabuck, A.D., Raghavachari, K., Foresman, J.B., Cioslowski, J., Ortiz, J.V., Stefanov, B.B., Liu, G., Liashenko, A., Piskorz, P., Komaromi, I., Gomperts, R., Martin, R.L., Fox, D.J., Keith, T.A., Al-Laham, M.A., Peng, C.Y., Nanayakkara, A., Gonzalez, V., Challacombe, M., Gill, P.M.W., Johnson, B.G., Chen, W., Wong, M.W., Andres, J.L., Head-Gordon, M., Replogle E.S. and Pople, J.A., Gaussian Inc., Pittsburgh, PA. 14, 1998.
27. Dauber-Osguthorpe, P., Roberts, V.A., Osguthorpe, D.J., Wolff, J., Genest, M. and Hagler, A.T., Proteins, 4 (1988) 31.
28. Andersen, H.C., J. Chem. Phys., 72 (1980) 2384.
29. Verlet, L., Phys. Rev., 159 (1967) 98.
30. Saunders, M., Houk, K.N., Wu, Y.-D., Still, W.C., Lipton, M., Chang, G. and Guida, W.C., J. Am. Chem. Soc., 112 (1990) 1419.
31. Vasquez, M., Meirovitch E. and Meirovitch, H., J. Phys. Chem., 98 (1994) 9380.
32. Richards, F.M., Annu. Rev. Biophys. Bioeng., 6 (1977) 151.
33. Allen, M.P., and Tildesley, D.J. (Ed.), Computer Simulation of Liquids, Clarendon Press, Oxford, UK, 1987, p. 204.
34. SPARTAN Version 5.1.3, Wavefunction, I.V.K.A., #370 Irvine, CA.
35. Boys, S.F. and Bernardi F., Mol. Phys., 19 (1970) 553.
36. Famulari, A., Specchio, R., Sironi, M. and Raimondi, M., J. Chem. Phys., 108 (1998) 3296.
37. Konko, N. and Dannenberg J.J., J. Phys. Chem. A, 105 (2001) 1944.